Stepwise Removal of the Copolymer Template from Mesopores and Micropores in SBA-15

Chia-Min Yang,*,† Bodo Zibrowius, Wolfgang Schmidt, and Ferdi Schüth

Max-Planck-Institut für Kohlenforschung, Kaiser-Wilhelm-Platz 1, D-45470 Mülheim an der Ruhr, Germany

Received March 19, 2004. Revised Manuscript Received April 23, 2004

A method for the removal of the triblock copolymer template from mesoporous silica SBA-15 in two stages has been developed. The mesopores of SBA-15 are first vacated by treatment with sulfuric acid that decomposes accessible portions of the template via ether cleavage. The concentration of the acid was found to be crucial for the decomposition of the template. The micropores of SBA-15 can then be vacated by calcination at 200 °C, a low temperature that prevents the silica matrix from shrinking, so that both the mesopores and the micropores retain their original sizes and volumes. The connectivity of the mesopores was studied by imaging the inverse platinum replicas of SBA-15 materials. The acid-treated SBA-15 materials also show less shrinkage, even when subsequently calcined at 540 °C. Compared with the template removal just by calcination, the stepwise removal of the copolymer template generates materials with wider mesopores and larger micropore volumes. Furthermore, this method opens up the possibility of functionalizing the mesopores and micropores independently, widening the field of application of copolymer-templated mesoporous silicas.

Introduction

The discovery of ordered mesoporous materials has sparked great interest owing to their potential applications in catalysis, in adsorption and separation processes, and as support for nanostructured materials with novel physical and chemical properties.[1−9] In 1998, a new synthesis pathway to large-pore mesoporous materials was found in which triblock poly(ethylene oxide)−poly(propylene oxide)−poly(ethylene oxide) ($EO_nPO_mEO_n$) copolymers act as structure-directing agents.[10,11] Such a route provides great opportunities for fine-tuning the pore dimensions and pore structures of mesoporous materials. For instance, mesoporous silica SBA-15, which is prepared with Pluronic P123 ($EO_{20}PO_{70}EO_{20}$, P123) as template, has a hexagonally arranged channel-type pore system. Variation of the synthesis conditions such as aging temperature or acid concentration allows the physicochemical properties of SBA-15 materials to be controlled.[12,13] Copolymer-templated mesoporous silicas generally have thicker walls than MCM-41-type materials and hence higher thermal and hydrothermal stabilities.

Recent studies have confirmed that micropores exist in the silica walls of the ordered mesopores of SBA-15.[12−17] The microporosity results from the mutually interpenetrating network of silica and hydrophilic EO chains formed during the assembly of the organic/inorganic hybrid material. The micropores can contribute to up to 30% of the total pore volume in SBA-15.[17] Such a bimodal pore structure consisting of mesoporous channels surrounded by microporous coronas is special in the sense that it provides an opportunity of depositing different functionalities or guest materials in either one or the other pore system. Hence, it is highly desirable to develop methods for vacating the two pore types not simultaneously, but in a stepwise fashion. The removal of the template P123 from as-synthesized SBA-15 is usually accomplished by calcination.[18] Other methods including microwave digestion,[19] solvent extraction,[12] and supercritical fluid extraction[20] have also been

* To whom correspondence should be addressed. E-mail: cmyang@platinum.chem.nthu.edu.tw.

† Present address: Department of Chemistry, National Tsing Hua University, Hsinchu, 300, Taiwan.

(1) Stein, A. *Adv. Mater.* **2003**, *15*, 763.
(2) Wight A. P.; Davis, M. E. *Chem. Rev.* **2002**, *102*, 3589.
(3) de A. A. Soler-Illia, G. J.; Sanchez, C.; Lebeau, B.; Patarin, J. *Chem. Rev.* **2002**, *102*, 4093.
(4) Davis, M. E. *Nature* **2002**, *417*, 813.
(5) Schüth, F.; Schmidt, W. *Adv. Mater.* **2002**, *14*, 629.
(6) Sayari A.; Hamoudi, S. *Chem. Mater.* **2001**, *13*, 3151.
(7) Ying, J. Y.; Mehnert C. P.; Wong, M. S. *Angew. Chem., Int. Ed.* **1999**, *38*, 56.
(8) Ciesla, U.; Schüth, F. *Microporous Mesoporous Mater.* **1999**, *27*, 131.
(9) Moller, K.; Bein, T. *Chem. Mater.* **1998**, *10*, 2950.
(10) Zhao, D.; Feng, J.; Huo, Q.; Melosh, N.; Fredrickson, G. H.; Chmelka, B. F.; Stucky, G. D. *Science* **1998**, *279*, 548.
(11) Zhao, D.; Huo, Q.; Feng, J.; Chmelka, B. F.; Stucky, G. D. *J. Am. Chem. Soc.* **1998**, *120*, 6024.
(12) Kruk, M.; Jaroniec, M.; Ko, C. H.; Ryoo, R. *Chem. Mater.* **2000**, *12*, 1961.
(13) Choi, M.; Heo, W.; Kleitz, F.; Ryoo, R. *Chem. Commun.* **2003**, 1340.
(14) Impéror-Clerc, M.; Davidson, P.; Davidson, A. *J. Am. Chem. Soc.* **2000**, *122*, 11925.
(15) Ryoo, R.; Ko, C. H.; Kruk, M.; Antochshuk, V.; Jaroniec, M. *J. Phys. Chem. B* **2000**, *104*, 11465.
(16) Ravikovitch, P. I.; Neimark, A. V. *J. Phys. Chem. B* **2001**, *105*, 6817.
(17) Galarneau, A.; Cambon, H.; Di Renzo, F.; Ryoo, R.; Choi, M.; Fajula, F. *New J. Chem.* **2003**, *27*, 73.
(18) Kleitz, F.; Schmidt, W.; Schüth, F. *Microporous Mesoporous Mater.* **2003**, *65*, 1.
(19) Tian, B.; Liu, X.; Yu, C.; Gao, F.; Luo, Q.; Xie, S.; Tu, B.; Zhao, D. *Chem. Commun.* **2002**, 1186.
(20) Van Grieken, R.; Calleja, G.; Stucky, G. D.; Melero, J. A.; Garcia, R. A.; Iglesias, J. *Langmuir* **2003**, *19*, 3966.

10.1021/cm049526z CCC: $27.50 © 2004 American Chemical Society
Published on Web 06/19/2004

investigated. However, all these methods clear both pore types simultaneously. Furthermore, the extraction-based methods fail to remove the P123 template completely.

Very recently, we have developed a method to empty the bimodal pore system in SBA-15 step by step.[21] The mesoporous channels are first vacated by decomposition of the triblock copolymer template via ether cleavage with sulfuric acid. In a second step, the occluded EO chains in the pore walls, which are not accessible to the acid, can be thermally decomposed to generate the microporosity. This method is advantageous for the design of advanced nanomaterials since it allows the surface of mesopores and micropores of SBA-15 to be modified with different functionalities. Template removal by acid treatment has also been applied to remove the P123 template from functionalized SBA-15.[22−25]

In this paper, we report in more detail on the influence of the experimental conditions of the acid treatment on the resulting SBA-15 materials. Our results show that SBA-15 materials prepared according to our method have larger mesopore diameters and micropore volumes than samples calcined directly. The inverse platinum replicas of these SBA-15 materials indicate that the degree of interconnectivity between mesopores is significantly enhanced. In addition, the treatment with sulfuric acid facilitates a further condensation of the silica matrix, which prevents the treated SBA-15 materials from shrinking significantly during subsequent calcination. These advantages make our method promising for the design of multifunctional materials based on mesoporous silica.

Experimental Section

Synthesis. SBA-15 materials were synthesized according to the reported procedure.[11] A hydrochloric acid solution of the triblock copolymer P123 was prepared, and tetraethoxysilane (TEOS) was then added. The molar composition was 1:5.9:193:0.017 TEOS:HCl:H_2O:P123. The mixture was stirred at 40 °C for 20 h, followed by aging at 60 or 90 °C for 24 h. The solid was filtered and dried at 80 °C overnight. For the treatment with sulfuric acid, 1.0 g of as-synthesized SBA-15 was mixed with 100 mL of 32−60 wt % H_2SO_4 solution and heated at 95 °C for 8−32 h. After the reaction, the products were washed with water until the eluent became neutral, then washed with acetone, and dried at 80 °C. Throughout this paper, the materials are referred to as Axx-yy-zz or Bxx-yy-zz, where A and B refer to different batches of as-synthesized SBA-15 used as starting materials, xx denotes the aging temperature in °C, yy denotes the weight percentage of H_2SO_4 in the solution, and zz denotes the duration of treatment with H_2SO_4 in hours. For example, A60-40-24 refers to a SBA-15 sample aged at 60 °C and treated with 40 wt % H_2SO_4 solution for 24 h. To remove the occluded EO chains in the silica walls, xx-48-24 samples were further heated for 6 h in air at 200 or 540 °C. These calcined samples are referred to as Axx-48-24-L or Axx-48-24-H, where L or H means further calcination at low (200 °C) or high (540 °C) temperature. SBA-15 materials calcined at 540 °C without any previous acid treatment are referred to as Axx-00-C. Platinum replicas of selective samples were prepared according to the procedure reported.[17] Typically, 0.2 g of SBA-15 was loaded with 0.18 g of tetraammine platinum(II) nitrate by repeated impregnation of its aqueous solution. The sample was dried at 100 °C and was then heated under hydrogen flow at 300 °C for 4 h. The silica was dissolved in 10% HF solution.

Characterization. Powder X-ray diffraction data (PXRD) were obtained on a Stoe STADI P diffractometer in reflection mode using Cu Kα radiation. Nitrogen sorption isotherms were measured at 77 K using a Micromeritics ASAP 2010 instrument. Each sample was evacuated at 80 °C for 12 h. The BET surface area was calculated from the adsorption branches in the relative pressure range of 0.05−0.20, and the total pore volume was evaluated at a relative pressure of 0.95. The pore diameter and the pore size distribution were calculated from the desorption branch using the Barrett−Joyner−Halenda (BJH) method. For t-plot analyses, the Harkins−Jura equation with standard parameters obtained from a nonporous reference material was used. Solid-state NMR spectra were measured on a Bruker Avance 500WB spectrometer using a 4-mm MAS probe at a spinning rate of 10 kHz. The experimental conditions for ^{13}C CP/MAS NMR were a recycle delay of 2 s, a number of scans between 20 000 and 32 000, contact time of 1 ms, and ^1H $\pi/2$ pulse of 4.4 μs. Those for ^{29}Si MAS NMR were a recycle delay of 30 s, 2800 scans, and a $\pi/4$ pulse of 2.2 μs. The TEM images were obtained with an Hitachi HF2000 electron microscope.

Results and Discussion

The physicochemical properties of the acid-treated SBA-15 materials were found to be strongly affected by the conditions of this treatment. The influence of the concentration of H_2SO_4 was studied first. Figure 1a shows a comparison of the PXRD patterns of the series of SBA-15 materials aged at 90 °C. All samples exhibit intense (100), (110), and (200) reflections in the small-angle region attributed to a hexagonal structure. The cell constants a for the hexagonal $p6mm$ structure of the acid-treated materials A90-32-24 and A90-48-24 are identical to that of as-synthesized SBA-15 (A90-00-00). On the other hand, the cell constants of A90-60-24 and A90-00-C are reduced by about 2% and 7%, respectively. The intensity of the (110) reflection of A90-00-C is slightly lower than that of the (200) reflection, while the opposite is true for acid-treated SBA-15 materials. In addition, the intensity ratios of the (110) and (200) reflections are higher for A90-32-24 and A90-48−24 than that for A90-60-24. For hexagonal mesoporous silicas, MCM-41[26−29] and SBA-15,[29,30] the relative intensities of these two reflections contain information on the thickness of the pore walls. However, these intensities are also affected by other factors including the density of the silica walls and the roughness of the mesopore surfaces.

Nitrogen sorption measurements also point to differences between the structural properties of the materials under study. All isotherms, shown in Figure 2a, exhibit sharp steps with hysteresis loops corresponding to the

(21) Yang, C. M.; Zibrowius, B.; Schmidt, W.; Schüth, F. *Chem. Mater.* **2003**, *15*, 3739.
(22) Yang, C. M.; Zibrowius, B.; Schüth, F. *Chem. Commun.* **2003**, 1772.
(23) Yang, C. M.; Wang, Y. Q.; Zibrowius, B.; Schüth, F. *Phys. Chem. Chem. Phys.* **2004**, *6*, 2461.
(24) Wang, Y. Q.; Yang, C. M.; Zibrowius, B.; Spliethoff, B.; Lindén, M.; Schüth, F. *Chem. Mater.* **2003**, *15*, 5029.
(25) Wang, Y. Q.; Zibrowius, B.; Yang, C. M.; Spliethoff, B.; Schüth, F. *Chem. Commun.* **2004**, 46.
(26) Feuston, B. P.; Higgins, J. B. *J. Phys. Chem.* **1994**, *98*, 4459.
(27) Kruk, M.; Jaroniec, M.; Sayari, A. *Chem. Mater.* **1999**, *11*, 492.
(28) Ågren, P.; Linden, M.; Rosenholm, J. B.; Schwarzenbacher, R.; Kriechbaum, M.; Amenitsch, H.; Laggner, P.; Blanchard, J.; Schüth, F. *J. Phys. Chem. B* **1999**, *103*, 5943.
(29) Sauer, J.; Marlow, F.; Schüth, F. *Phys. Chem. Chem. Phys.* **2001**, *3*, 5579.
(30) Zholobenko, V. L.; Khodakov, A. Y.; Durand, D. *Microporous Mesoporous Mater.* **2003**, *66*, 297.

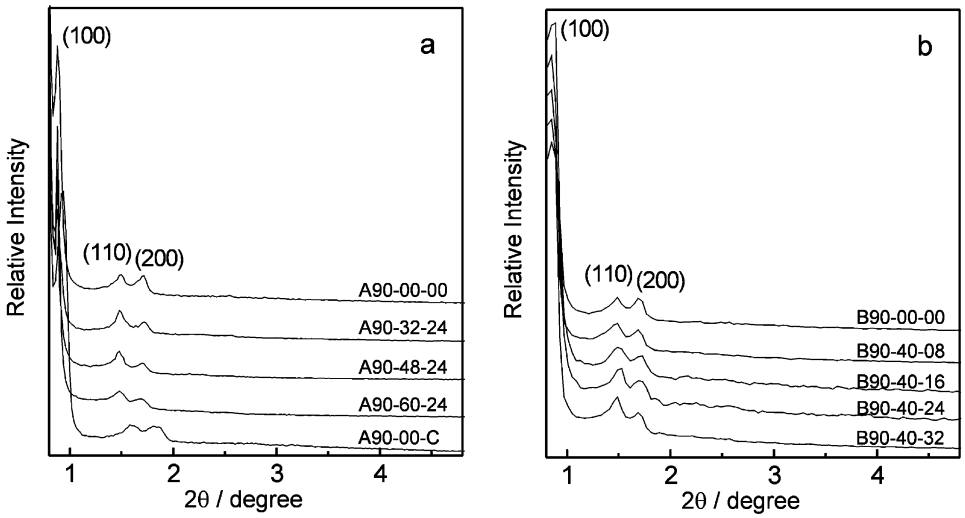

Figure 1. (a) PXRD patterns of SBA-15 materials: as-synthesized, treated with H_2SO_4 of different concentrations, and calcined. (b) PXRD patterns of SBA-15 materials: as-synthesized and treated with 40 wt % H_2SO_4 for different times.

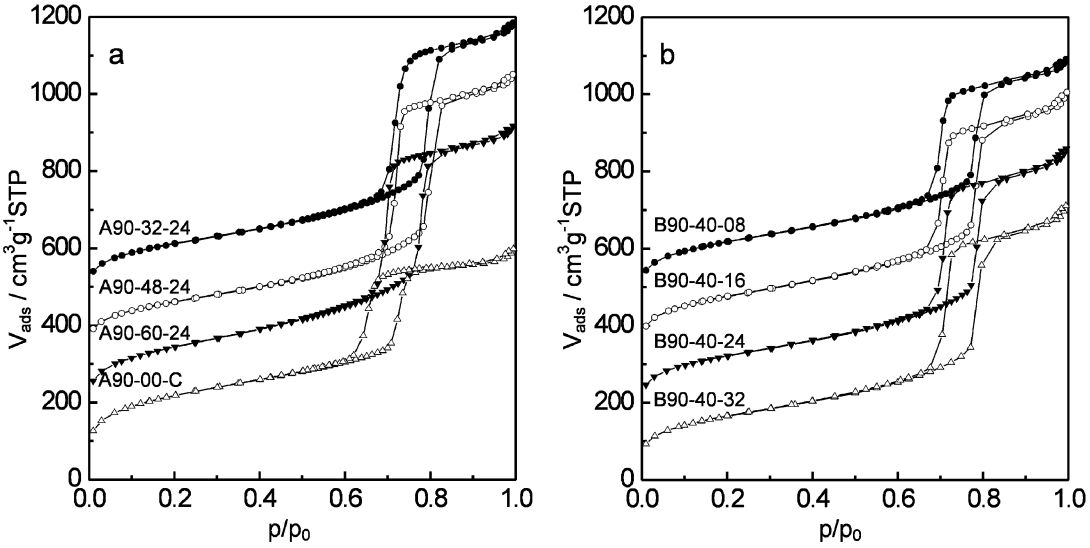

Figure 2. (a) Nitrogen sorption isotherms of SBA-15 materials after treatment with H_2SO_4 of different concentrations or calcination. (b) Nitrogen sorption isotherms of SBA-15 materials after treatment with 40 wt % H_2SO_4 for different times. The isotherms in (a) and (b) are shifted by 0, 150, 300, and 450 cm^3 g^{-1} STP, respectively.

filling of the ordered mesopores. Whereas the positions and the widths of the hysteresis loops for A90-32-24 and A90-48-24 are almost identical, the hysteresis loop for the sample treated with H_2SO_4 of higher concentration (60 wt %) is shifted to lower relative pressure. However, this shift is less pronounced than that found for the calcined material (A90-00-C). The physicochemical properties of these materials derived from the sorption and PXRD measurements are summarized in Table 1. Comparing the acid-treated samples, it is found that A90-60-24 has thicker pore walls and smaller pores than the samples treated with less concentrated H_2SO_4, which have nearly identical cell constants. However, the properties of the calcined material (A90-00-C) deviate substantially from those of the acid-treated ones: of this series of samples, it has the smallest cell constant, the smallest pore diameter, but the thickest pore walls. As Table 1 shows, similar trends of these physicochemical parameters are observed for the SBA-15 materials aged at 60 °C.

The influence of the duration of the acid treatment on the structural properties of SBA-15 materials was also investigated. New batches of SBA-15 materials aged at 60 and 90 °C were prepared for the study and an acid concentration of 40 wt % was used. Figure 1b shows PXRD patterns of the series of SBA-15 materials aged at 90 °C. The cell constants of all the materials are the same, while the relative intensities of the (110) and (200) reflections increase on extending the duration of the acid treatment. Pore diameters and pore volumes were derived from the nitrogen sorption isotherms shown in Figure 2b. The maximum values of the pore diameter and the pore volume (cf. Table 1) are not reached until the acid treatment has been carried out for at least 24 h, suggesting that under these reaction conditions (40 wt % H_2SO_4 at 95 °C) such a long time is necessary to remove the polymer from the mesopores completely. For B90-40-08 and B90-40-16, the remaining fragments of the template result in smaller pore diameters and pore volumes, and they may also contribute to the lower intensities of the (110) and (200) reflections due to the lower diffraction contrast. For the SBA-15 materials aged at 60 °C, the same conclusions can be drawn from the data compiled in Table 1.

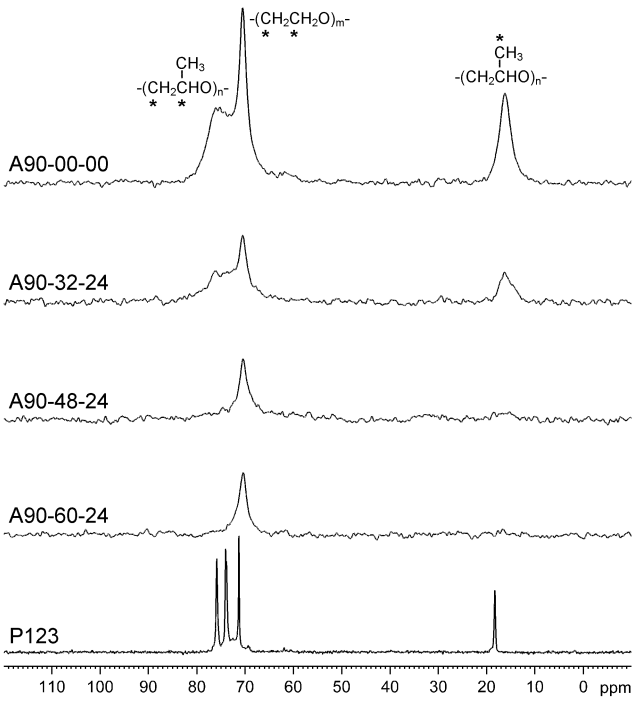

Figure 3. ^{13}C CP/MAS NMR spectra of as-synthesized SBA-15 aged at 90 °C and SBA-15 materials after treatment with H_2SO_4 of different concentrations for 24 h. The bottom trace gives the spectrum of neat P123.

Table 1. Physicochemical Properties of SBA-15 Materials after Treatment with H_2SO_4 or Calcination[a]

sample	a_o (nm)	D_{BJH} (nm)	t_w (nm)	V ($cm^3\,g^{-1}$)	S_{BET} ($m^2\,g^{-1}$)
A90-32-24	11.8	8.1	3.7	1.01	583
A90-48-24	11.8	8.1	3.7	1.03	599
A90-60-24	11.6	7.4	4.2	1.02	608
A90-00-C	11.0	5.8	5.2	0.86	578
A90-48-24-L	11.8	8.1	3.7	1.05	590
A90-48-24-H	11.5	6.9	4.6	0.95	575
A60-32-24	11.0	7.1	3.9	0.78	500
A60-48-24	11.0	7.1	3.9	0.84	522
A60-60-24	10.8	6.8	4.0	0.84	524
A60-00-C	9.6	4.7	4.9	0.47	463
A60-48-24-L	11.0	7.1	3.9	0.89	516
A60-48-24-H	10.7	6.2	4.5	0.70	499
B90-40-08	11.8	6.8	5.0	0.90	482
B90-40-16	11.8	7.4	4.4	0.93	527
B90-40-24	11.8	8.1	3.7	1.01	586
B90-40-32	11.8	8.1	3.7	1.01	593
B60-40-08	11.0	6.2	4.8	0.74	405
B60-40-16	11.0	6.7	4.3	0.76	494
B60-40-24	11.0	7.1	3.9	0.83	511
B60-40-32	11.0	7.1	3.9	0.84	520

[a] a_o: cell constant; D_{BJH}: pore diameter calculated from the desorption branch; t_w: pore wall thickness; V: total pore volume; S_{BET}: BET surface area.

The influence of different experimental conditions such as acid concentrations and durations of the treatment on the decomposition of the P123 template was investigated by ^{13}C CP/MAS NMR. The spectra of the series of materials treated with H_2SO_4 of different concentrations are shown in Figure 3.

Whereas the line at 16.3 ppm can easily be assigned to the methyl groups of the PO units, the lines of the carbons in the main chains of the PO and EO blocks overlap. The NMR spectra of both bulk PEO[31] and PPO[32] are rather complex. Therefore, a ^{13}C CP/MAS NMR spectrum of neat P123 was measured under the same experimental conditions as those applied for the SBA-15 materials. The well-resolved lines in the spectrum (Figure 3, bottom) can be assigned to the methine carbons (75.9 ppm), the methylene carbons (74.1 and 73.5 ppm), and the methyl carbons (18.3 ppm) of the PO units[32] and to the methylene carbons (71.3 ppm) of the EO units.[31] With the low spectral resolution obtained for the materials under study, the most intense line at 70.5 ppm is attributed to the EO units and the less defined broad lines with a maximum between 73 and 76 ppm to the chain carbons of the PO units. After treatment with H_2SO_4 for 24 h, all the lines of P123 decrease in intensity. Furthermore, if all the PO blocks are to be removed from the material, the concentration of the acid must be at least 48 wt %. The survival of EO chains in the samples is thought to result from the protection of occluded EO chains by the silica matrix, preventing them from cleavage by H_2SO_4.[21]

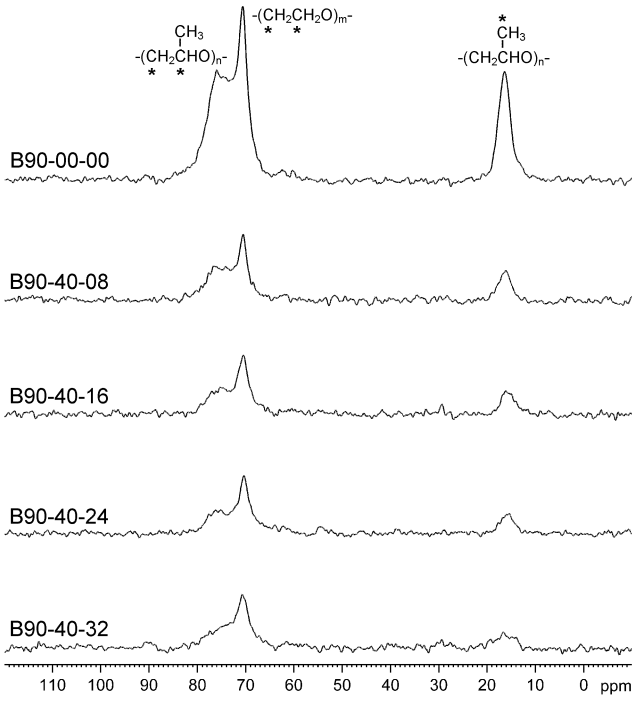

Figure 4. ^{13}C CP/MAS NMR spectra of as-synthesized SBA-15 aged at 90 °C and SBA-15 materials after treatment with 40 wt % H_2SO_4 for different times.

Figure 4 shows ^{13}C CP/MAS NMR spectra of the series of the SBA-15 materials treated with 40 wt % H_2SO_4 for different durations. The slight differences between the spectra of A90-00-00 in Figure 3 and B90-00-00 in Figure 4 may be attributed to small differences in the preparation and product recovery (that is, filtration and washing). After treatment for only 8 h, the lines attributed to both the PO and the EO units are significantly decreased. However, the spectra show that even after treatment for 32 h, some PO units are still present in the material, suggesting that the concentration of H_2SO_4 rather than the duration of the treatment is crucial for the removal of the P123 template from SBA-15. On the other hand, nitrogen sorption analysis suggests that complete removal of the template from

(31) Harris, D. J.; Bonagamba, T. J.; Hong, M.; Schmidt-Rohr, K. *Macromolecules* **2000**, *33*, 3375.
(32) Chisholm, M. H.; Navarro-Llobet, D. *Macromolecules* **2002**, *35*, 2389.

Table 2. Parameters of the Gaussian Lines[a] Used for the Deconvolution of the ^{29}Si NMR Spectra in Figure 5

	Q^2			Q^3			Q^4		
sample	δ (ppm)	$\Delta\nu_{1/2}$ (Hz)	I (%)	δ (ppm)	$\Delta\nu_{1/2}$ (Hz)	I (%)	δ (ppm)	$\Delta\nu_{1/2}$ (Hz)	I (%)
A90-00-00	−91.0	600	7	−100.9	600	40	−110.3	760	53
A90-32-24	−91.4	620	5	−101.4	620	32	−110.9	790	63
A90-48-24	−91.9	620	4	−101.4	620	31	−111.0	790	65
A90-60-24	−90.9	490	6	−101.2	620	28	−110.8	790	66
A90-00-C	−91.4	780	6	−100.8	780	30	−108.8	980	64
A90-48-24-H	−91.4	780	3	−101.2	780	25	−109.8	980	72

[a] δ: chemical shift; $\Delta\nu_{1/2}$: full-width at half-height; I: relative intensity.

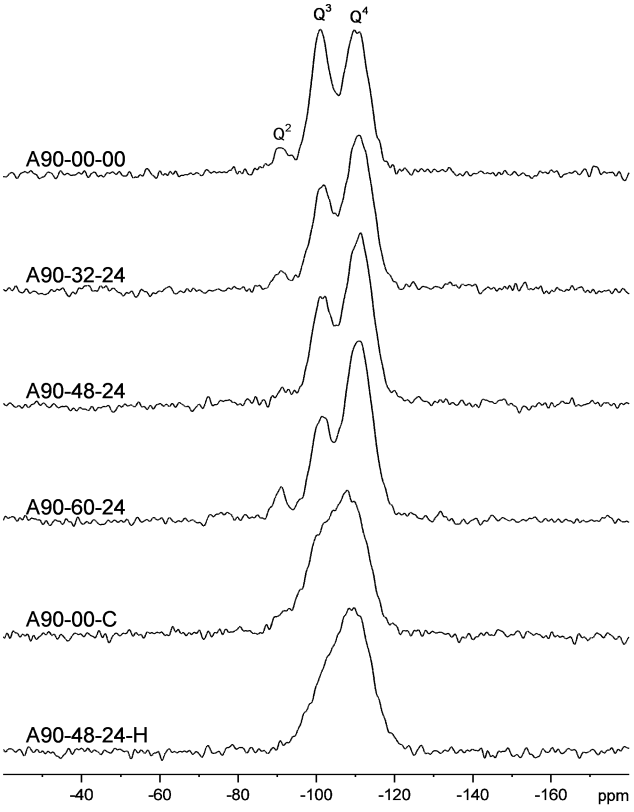

Figure 5. ^{29}Si MAS NMR spectra of selected SBA-15 materials aged at 90 °C.

the mesopores occurs after acid treatment for 24 h. Apparently, the residual template does not affect the determination of the pore diameter. For B90-40-08 and B90-40-16, the remaining amounts of the template are larger, resulting in smaller pore diameters and pore volumes.

The treatment with H_2SO_4 to decompose the template in as-synthesized SBA-15 also affects the chemical properties of the silica matrix. Figure 5 shows ^{29}Si MAS NMR spectra of as-synthesized, acid-treated, and calcined SBA-15. These spectra were deconvoluted[33] and the positions, widths, and intensities of the lines attributed to the various Q^n groups ($Si(OSi)_n(OH)_{4-n}$, n = 2,3,4) are summarized in Table 2. The comparison of the spectra indicates that after treatment with H_2SO_4 at 95 °C the Q^4 line is enhanced and the Q^2 and Q^3 lines are weakened, suggesting that this procedure facilitates the condensation reaction of the silanol groups in the silica matrix. This condensation can be expected under such strongly acidic conditions. However, the intensities of the Q^3 lines are still high after the acid treatment, reflecting the high concentration of silanol groups in these materials. Furthermore, when 60 wt % H_2SO_4 is used, the Q^2 line is even more pronounced than after treatment with less concentrated acid. As indicated by the results of PXRD and sorption analyses, A90-60-24 has a somewhat smaller cell constant and significantly narrower pores than the materials treated with less concentrated H_2SO_4. Therefore, the relatively intense and narrow Q^2 line for A90-60-24 might reflect rearrangements in the silica matrix during the shrinkage of the material to release the structural strain. The spectra of the two materials calcined at 540 °C are also given in Figure 5. Both spectra show broad asymmetric lines. Although the deconvolution of these structureless lines is clearly less reliable than that of the other spectra, the concentration of Q^2 and Q^3 species in A90-48-24-H is significantly lower than that in the material that was not treated with acid prior to calcination. Hence, the acid-catalyzed condensation can be used to influence the structure and the properties of the silica matrix.

All the SBA-15 materials obtained after treatment with H_2SO_4 contain almost no micropores,[21] but the subsequent calcination decomposes the EO chains occluded in the silica walls and vacates the micropores. Figure 6 compares the t-plots of SBA-15 calcined directly with those of acid-treated materials before and after calcination at 200 or 540 °C. The t-plots of SBA-15 aged at 60 °C give straight extrapolation lines between t = 0.50 and t = 0.75 nm, while for the 90 °C-aged SBA-15 the t-plots give straight lines between t = 0.50 and t = 0.80 nm. These lines intercept the y-axis at different levels above the origin, indicating different micropore volumes in these materials. The derived micropore volumes are summarized in Table 3. For both the acid-treated SBA-15 materials (A60-48-24 and A90-48-24) the calculated micropore volumes are 0.04 cm^3 g^{-1}, slightly larger than the values derived from argon sorption measurements.[21] This deviation may be attributed to the different properties of the probe molecules used[34] and also to the choice of the reference material for the t-plot analysis. In general, the micropore volumes of the SBA-15 materials treated with acid and then calcined at 200 °C are about twice as large as those of samples calcined directly at 540 °C. Even if the acid-treated SBA-15 materials are calcined at 540 °C, the micropore volumes are still significantly larger than those in the samples that were just calcined.

(33) Massiot, D.; Fayon, F.; Capron, M.; King, I.; Le Calvé, S.; Alonso, B.; Durand, J.-O.; Bujoli, B.; Gan, Z.; Hoatson, G. *Magn. Reson. Chem.* **2002**, *40*, 70.

(34) de Boer, J. H.; Linsen, B. G.; Osinga, T. J. *J. Catal.* **1965**, *4*, 643.

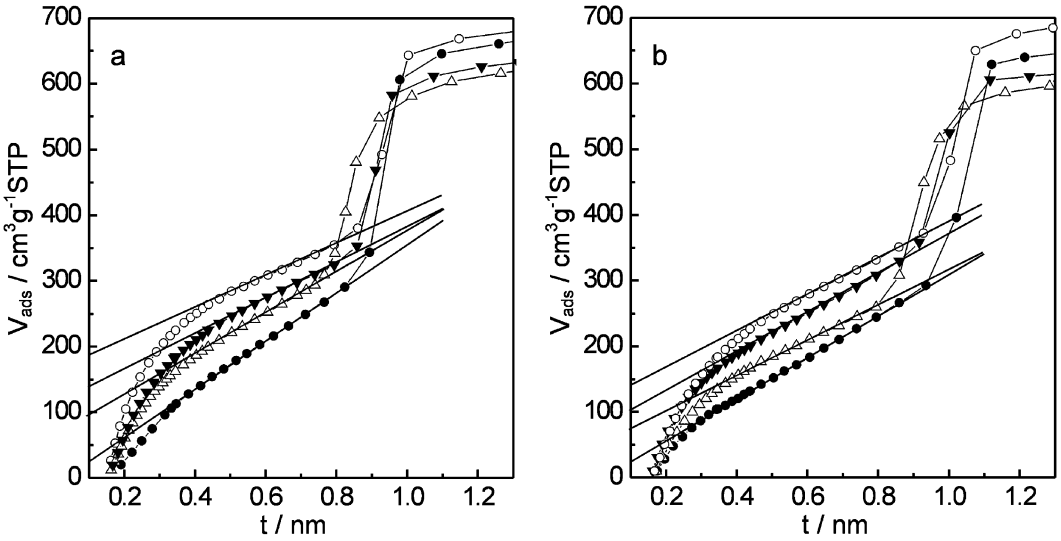

Figure 6. t-plots of SBA-15 materials: Axx-48-24 (●), Axx-48-24-L (○), Axx-48-24-H (▼), and Axx-00-C (△), where xx is 60 (a) or 90 (b).

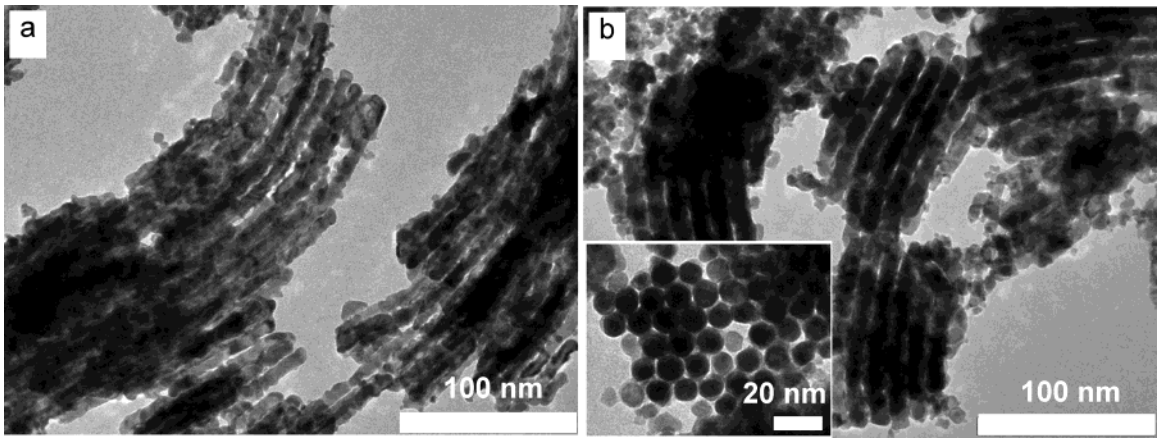

Figure 7. TEM images of inverse Pt replicas of A90-00-C (a) and A90 48 24 L (b) viewed perpendicular to the nanowire axis. Inset in (b) shows the image of the inverse replica of A90-48-24-L viewed along the nanowire axis.

Table 3. Influence of Calcination on the Micropore Volume of SBA-15

	micropore volume/cm^3g^{-1}	
sample	xx= 60	xx=90
Axx-48-24	0.04	0.04
Axx-48-24-L	0.29	0.22
Axx-48-24-H	0.21	0.16
Axx-00-C	0.15	0.12

To image the pore structure, inverse Pt replicas of selected SBA-15 materials were prepared and the host silicas were dissolved in dilute HF. Figure 7 shows the TEM images of the inverse replicas of A90-00-C and A90-48-24-L. Both show bundles of Pt nanowires, which reflect the mesoporous channels and the bridges interconnecting the channels in the host SBA-15 materials.[17] The average diameter of the Pt nanowires in the inverse replica of A90-00-C is about 6.5 nm, while that of the nanowires produced from A90-48-24-L is about 9.0 nm. Both values are larger than the pore diameters of the host silicas derived from nitrogen sorption measurements (Table 1). To judge the significance of this finding, one has to take into account that the pore diameters derived from desorption branches using the BJH method are usually underestimated.[16] Bridges of 2.5−4.5 nm in diameter among Pt nanowires are observed for the inverse replica of A90-00-C. For A90 48 24 L, wider bridges (3.5−6.0 nm in diameter) are observed and the number of bridges is higher than that for A90-00-C. The Pt nanowires are hexagonally ordered, and the images viewed along the nanowire axis (inset in Figure 7) show that most of the nanowires have hexagonal cross sections. However, one should be aware that the inverse Pt replicas are not exact mirror images of the pore structures of the host silicas.

TEM images of the inverse Pt replicas of the SBA-15 aged at 60 °C (A60-00-C and A60-48-24-L) are shown in Figure 8. The diameters of the Pt nanowires in both replicas are smaller than those observed for replicas of SBA-15 aged at 90 °C. For the inverse replica of A60-00-C, most of the Pt nanowires are not connected and are randomly packed. This might be due to the fact that the pore walls of the host silica A60-00-C only have pores with diameters smaller than 2.0 nm. The preparation of Pt replicas does not guarantee the preservation of such narrow bridges during the decomposition and reduction of the platinum complexes.[17] Our observation is consistent with previous reports, which showed that no significant connections between structural mesopores could be detected for calcined SBA-15 aged at 60 °C.[17] On the other hand, the inverse replica of A60-48-24-L

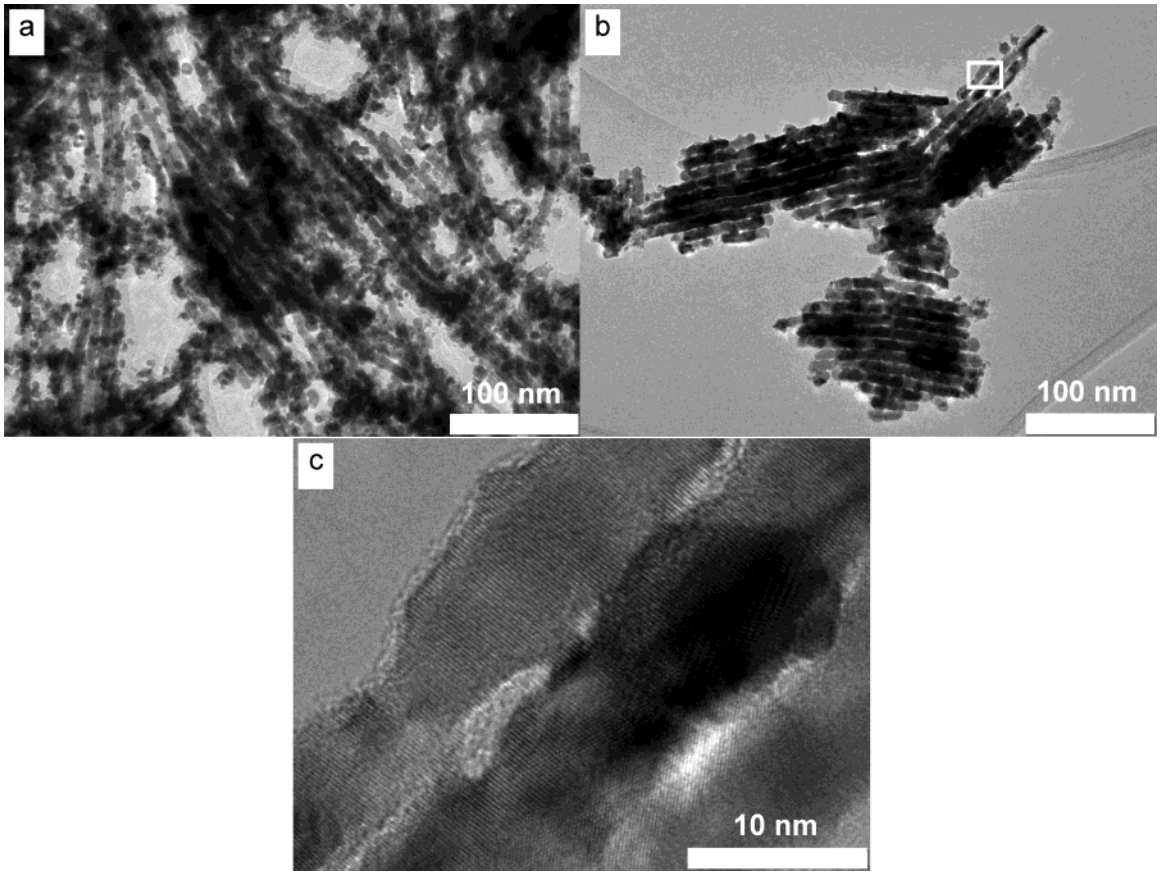

Figure 8. TEM images of inverse Pt replicas of A60-00-C (a) and A60-48-24-L (b). (c) Magnification of the rectangle area in (b).

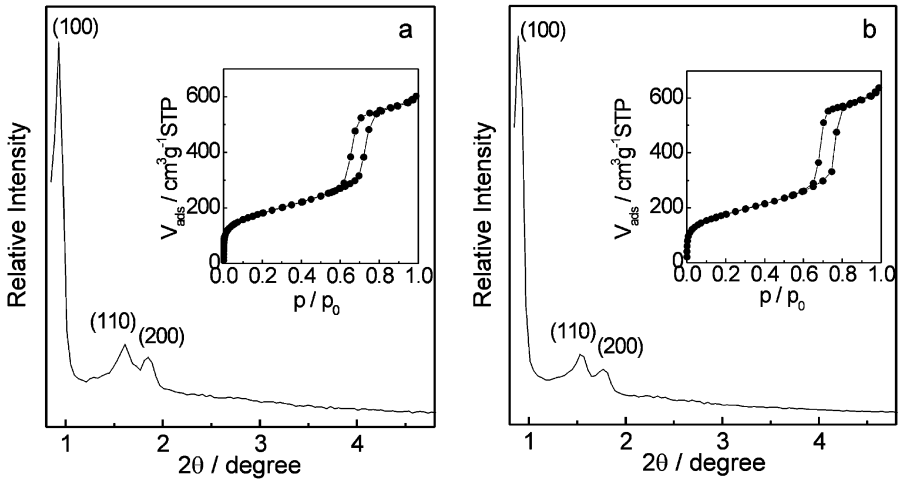

Figure 9. PXRD patterns and nitrogen sorption isotherms of A60-48-24-H (a) and A90-48-24-H (b).

shows ordered Pt nanowires interconnected with bridges of 2.5−5.0 nm in diameter, and some of the bridges could be resolved to be single-crystalline from one Pt nanowire to the other (Figure 8c). The observation indicates that, in addition to the micropores that could not be imaged by Pt replication, the host silica A60-48-24-L has a significant proportion of bridges with diameters larger than 2.0 nm in the pore walls. The differences between the inverse Pt replicas of A60-00-C and A60-48-24-L may be a further result of different degrees of shrinkage of the host SBA-15 materials during the calcination.

As shown above, subsequent calcination of the acid-treated SBA-15 at 540 °C leads to further condensation of the silica matrix and a decrease in the microporosity. Its influence on the mesoscopic structure of acid-treated SBA-15 materials was also studied. Figure 9 shows the PXRD patterns and nitrogen sorption isotherms of A60-48-24-H and A90-48-24-H materials. Both materials show characteristics of a highly ordered hexagonal structure. The positions of their X-ray reflections shift slightly toward larger angles compared to those of the parent acid-treated materials, indicating small shrinkages during calcination. The intensity ratios of the (110) and (200) reflections of these materials are significantly larger than those of samples directly calcined at 540 °C. Nitrogen sorption isotherms of A60-48-24-H and A90-48-24-H show sharp steps, which correspond to a narrow pore size distribution. In Figure 10, the pore diameters

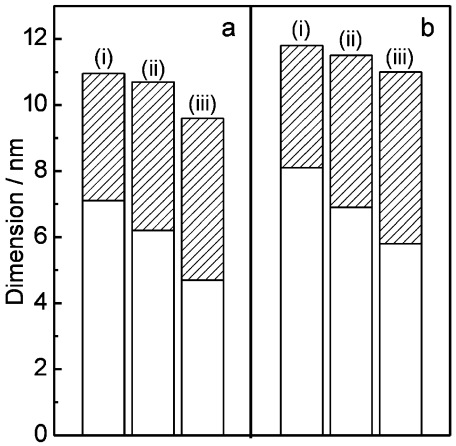

Figure 10. Comparison of pore diameters (height of the open area), cell constants (the total height), and pore wall thicknesses (height of the dashed area) of the SBA-15 materials: Axx-48-24-L (i), Axx-48-24-H (ii), and Axx-00-C (iii), where xx is 60 (a) or 90 (b).

and cell constants as well as the resulting pore wall thicknesses are compared with those of other SBA-15 materials. It is obvious that the acid-treated materials that are calcined at only 200 °C have the largest cell constants and pore diameters but the thinnest pore walls. After calcination at 540 °C, the pore walls of the materials (A60-48-24-H and A90-48-24-H) become thicker, accompanied by shrinkages of the pores. The materials calcined directly (A60-00-C and A90-00-C), on the other hand, have the smallest pore parameters and pore diameters but the thickest pore walls. The comparison clearly shows that the H_2SO_4 treatment preserves the original dimensions of the mesopores in the materials, and it also prevents the materials from shrinking significantly during subsequent calcination at higher temperatures.

Conclusions

Detailed studies have been conducted on the stepwise removal of copolymer template from SBA-15 by sulfuric acid treatment followed by calcination. The concentration of the sulfuric acid has been found to be crucial for the ether cleavage reaction. Residual template in the silica walls can completely be removed by calcination at very low temperature (200 °C). The SBA-15 materials prepared by this method have larger mesopore diameters and micropore volumes than the samples calcined directly. TEM images of Pt replicas of SBA-15 aged at 60 °C show that the mesopore connectivity is higher after stepwise removal of the template than after direct calcination. In addition, the acid-treated SBA-15 materials undergo less shrinkage during calcination at 540 °C. The method presented in this report provides the means of functionalizing the surfaces of mesopores and micropores independently and differently, making new applications of triblock copolymer-templated mesoporous silica materials possible.

Acknowledgment. The authors are indebted to Mr. Bernd Spliethoff for TEM characterization and Dr. Richard Mynott for many valuable comments on the manuscript.

CM049526Z